

## Rapid Communication

# Quantum Evaporation from Superfluid $^4\text{He}$

C.D.H. Williams

*School of Physics, University of Exeter, Exeter, EX4 4QL, U.K.*

*The quantum evaporation experiments of Brown and Wyatt<sup>2</sup> have been re-analysed in the light of a recent measurement of the high-energy phonon spectrum created by a pulse-heated thin film<sup>10</sup>. Two sources of systematic error become significant at the level of the precision required by this new analysis: firstly, in the detector position which is recalibrated by using large-angle roton evaporation; and secondly, in the liquid height due to capillary action affecting the level-detectors. These effects have been included in an improved simulation of the experiment which has brought the angular dependence of the measured and theoretical phonon-atom evaporation results into agreement within the mechanical tolerances of the apparatus. The re-analysis suggests that the roton-atom evaporation probability increases with wave vector.*

*PACS numbers: 67.40.Db, 68.45.Da, 67.40.-w*

## 1. INTRODUCTION

Although the mechanism known as *quantum evaporation*, in which a single atom is ejected from the free surface of superfluid  $^4\text{He}$  by the annihilation of a single phonon or roton in the liquid, was proposed several decades ago<sup>1</sup> the measurement<sup>2-5</sup> and calculation<sup>6-8</sup> of evaporation probabilities are both still problematic. The most comprehensive series of experiments on quantum evaporation to-date were reported by Brown and Wyatt<sup>2,9</sup> (BW). They used a time-of-flight method to investigate how the angular distribution of atoms detected by a bolometer depends on the incident angle of ballistic-excitation beams (phonons and rotons) directed at the liquid-vacuum surface (figure 1). They confirmed that a single excitation in the liquid, with wave vector  $q$  at angle of incidence  $\theta_h$  to the surface, could evaporate a single atom, with wave vector  $k$  at angle  $\phi_b$ , subject to the boundary conditions

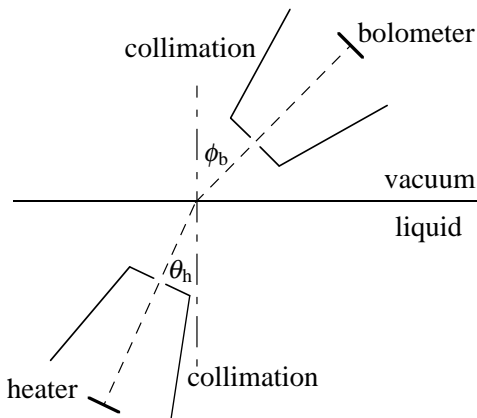


Fig. 1. Schematic diagram of a quantum evaporation experiment. The dashed line shows the path of the excitations.

$$E(q) - E_B = \frac{\hbar^2 k^2}{2m} \quad \text{and} \quad q \sin \theta_h = k \sin \phi_b \quad (1,2)$$

where  $E(q)$  is the  ${}^4\text{He}$  excitation spectrum and  $E_B/k_B = 7.15 \text{ K}$  is the binding energy of an atom, mass  $m$ , to the liquid surface at  $T = 0 \text{ K}$ . The BW experiments put an upper bound of  $\Delta k < 0.1 \text{ \AA}^{-1}$  on the size of any other quasiparticles involved in the evaporation, and concluded that only processes in which a single excitation was annihilated ejecting a single atom had been observed.

This paper describes a re-analysis of the BW experiment using a refined simulation that incorporates both a subsequent discovery<sup>10</sup> and hindsight. Two sources of systematic error become significant at the level of the precision attainable: firstly, in the detector position which is recalibrated by using large-angle roton evaporation; and secondly, in the liquid height due to the capillary action affecting the level-detectors. These corrections bring the BW measurements into *quantitative* agreement with the quantum evaporation model. The precision of the agreement opens the possibility that BW measurements can be used to test recent theories<sup>11,12</sup> that quantum evaporation by rotons has a strong wave-vector dependence.

## 2. PHONON EVAPORATION EXPERIMENTS

The BW simulation of the phonon-atom evaporation signals assumed that the excitations had a thermal distribution of energies (similar to equation 5) and radiated isotropically into the half-sphere in front of the heater before being collimated. Their simulated phonon-atom signals have a peak-height distribution  $P(\phi_b)$  much wider than the measured results. The phonons used in quantum evaporation experiments are generated by electrically pulsing a thin-film gold heater. It is now known<sup>10</sup> that this generates a beam of almost-parallel high-energy phonons with an approximately Gaussian distribution of energies centred on  $E/k_B = 10.2 \text{ K}$ , width  $\Delta E/k_B \sim 0.3 \text{ K}$ .

Incorporating these distributions into the simulation reduces the discrepancy with experiment but the agreement in the cases  $\theta_h = 75^\circ$  and  $80^\circ$  is not yet satisfactory. This is because the liquid level was a small distance below the point reported.

BW filled their cell with liquid helium while pulse-heating a thin ( $15\mu\text{m}$ ) wire running horizontally between two cylindrical posts (figure 2); the evaporated flux of atoms from the superfluid film dropped dramatically at the point the wire was just covered by bulk liquid. No corrections for capillary effects were made at the time but they are significant as the capillary constant<sup>13</sup> for  $^4\text{He}$  at low-temperatures is  $a = 0.706\text{mm}$ , assuming a value for the surface tension<sup>14</sup> of  $\sigma_0 = 3.54 \times 10^{-4}\text{Nm}$ .

In general, the height  $z$  of the meniscus midway between two vertical cylinders, radius  $r$  has to be calculated numerically, although tables<sup>15</sup> cover the case when  $z \gg r$ . A preliminary calculation of the surface profile indicated that the presence of the posts would raise the level at the centre of the wire by about  $0.15\text{mm}$ . This does reduce the discrepancy between simulation and experiment in the cases  $\theta_h = 75^\circ$  and  $80^\circ$  but the agreement is still unsatisfactory. The calculation had also indicated that accurate surface profiles are neither quick nor easy to determine numerically so, to investigate the detailed behaviour of the level-detector, a 3.7:1 scale model was built from brass components. The helium was represented by lubricating oil – it wets brass and has a capillary constant a factor of 3.7 times that of liquid helium. The assembly was placed in an oil bath on a level surface-plate. The absolute height of any point on the surface could be determined using a vernier height-gauge fitted with a sharp vertical point. The oil level was slowly raised and lowered, avoiding ripples, while watching the surface between the posts. As the level rose, at the point when the unperturbed distant surface was  $0.95 \pm 0.05\text{mm}$  lower than the wire, there was a sudden change; the meniscus swept along the wire, starting from the posts, leaving it entirely covered. Evidently the BW level-detectors overstated the height by  $\sim 0.25\text{mm}$  and correcting this brings the experiment and simulation into agreement for phonons (figure 3). The residual discrepancy for the larger heater angles is within the range allowed by the mechanical tolerances of the apparatus.

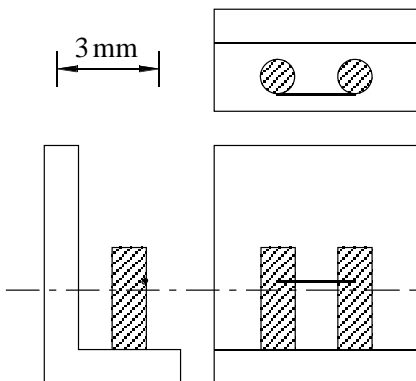


Fig. 2. Details of the BW level-detector with relevant features drawn to scale. The chained line indicates the critical level,  $0.25\text{mm}$  below the resistance wire joining the posts.

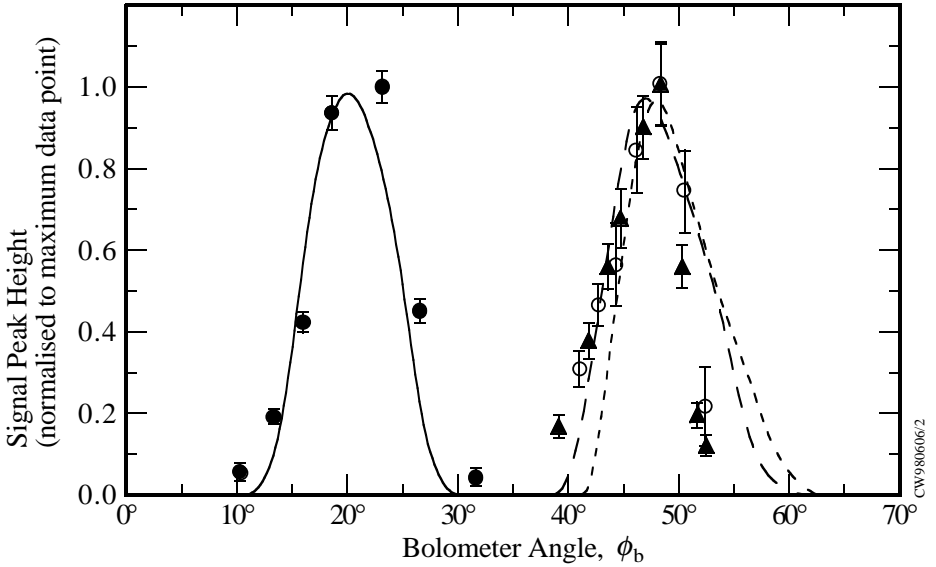


Fig. 3. Measured (points) and simulated (curves) angular dependence of the signal peak height  $P(\phi_b)$  for phonon $\rightarrow$ atom experiments with  $\theta_h=25^\circ$  (full circles, solid curve),  $75^\circ$  (full triangles, long dashes), and  $83^\circ$  (open circles, short dashes). Each curve is normalised to the maximum data point. The simulation places the liquid surface 0.25 mm below the nominal level given by BW.

The BW experiments (figure 1) had a mechanical precision of about 0.1 mm and an angular resolution of  $\sim 1^\circ$ . The heater–surface and surface–bolometer path lengths were both nominally 6.5 mm. Measurements with the free liquid surface below the level of the heater, which create direct (*i.e.*  $\theta_h \sim \phi_b$ ) atom beams by evaporating some of the superfluid film, indicated that there was a systematic angular error of  $\Delta\theta_h + \Delta\phi_b = 4^\circ$  where

$$\theta_h^{\text{True}} = \theta_h^{\text{Measured}} - \Delta\theta_h, \quad \phi_b^{\text{True}} = \phi_b^{\text{Measured}} - \Delta\phi_b. \quad (3,4)$$

BW adjusted their phonon data (BW figure 6 and the points in figure 3 above) for this angular error using this information because when  $\theta_h \sim \phi_b$  the adjustment depends only on the value of  $\Delta\theta_h + \Delta\phi_b$ .

### 3. ROTON EVAPORATION EXPERIMENTS

As the separate values of  $\Delta\phi_b$  and  $\Delta\theta_h$  were unknown, the roton-evaporation measurements (BW figures 8 and 11) were published without adjustment for the  $4^\circ$

angular error. However, having corrected the liquid level, it is now possible to deduce the distribution of the  $4^\circ$  error between  $\Delta\phi_b$  and  $\Delta\theta_h$ , as follows.

In one of the roton-evaporation experiments (BW figure 11) the bolometer was fixed at  $\phi_b^{\text{Measured}} = 75^\circ$  and the heater angle was varied. The integrated signal energy in this case has a well-defined peak at  $\theta_h = 20^\circ$  which, simulations prove, is insensitive to both the liquid level and bolometer angle but does depend on the heater angle, and hence  $\Delta\theta_h$ . Systematic comparison of the experimental data<sup>2,9</sup> with simulations has shown that  $\Delta\theta_h$  must be less than the random error in measuring the angles and therefore the systematic error in angle arises almost entirely from the  $\Delta\phi_b$  contribution; the data in figures 4 and 5 have had this correction applied and the simulation now broadly agrees with the measurements.

A  $4^\circ$  error in  $\phi_b$  corresponds to the bolometer being misplaced by  $\sim 0.45\text{mm}$ , about half its intended active width. This is considerably larger than the mechanical tolerances and it is likely that the bolometer was not, as has generally been assumed with this type of device, equally responsive over its entire area. Given its method of construction (a serpentine track of thin-film zinc) and operation (biased into a mixture of normal and superconducting domains) this seems a plausible explanation and clearly needs to be considered when designing future experiments.

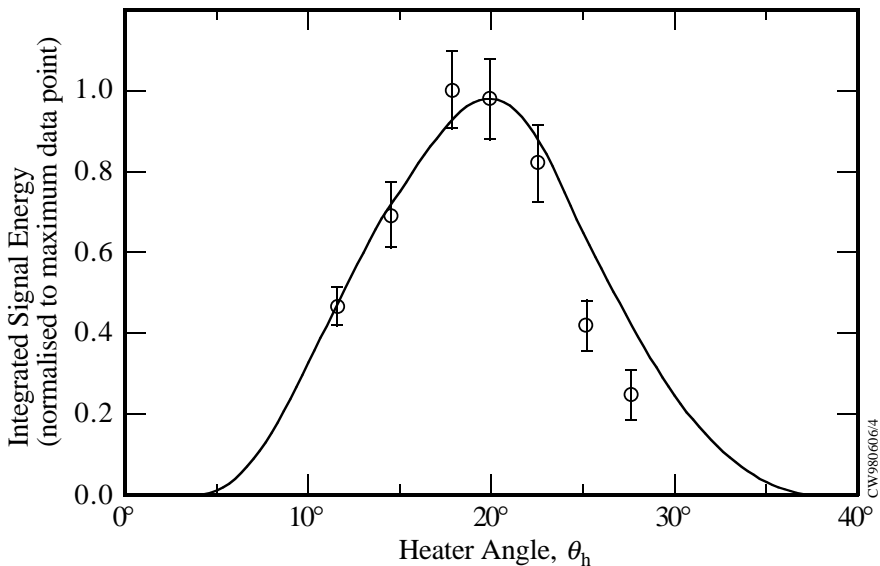


Fig. 4. The dependence of the integrated  $R^+ \rightarrow \text{atom}$  signal energy on heater angle for a bolometer at  $\phi_b^{\text{True}} = 71^\circ$ . The signals are integrated up to  $150\mu\text{s}$  after the start of the heater input pulse. The points are experiments using heater power  $-24\text{dB}$ . The curve is a simulation using  $T_{\text{eff}} = 1.5\text{K}$ .

#### 4. ROTON EVAPORATION PROBABILITIES

The residual discrepancy between model and experiment is relatively small and apparently affects (figure 5) roton-evaporated atoms detected at large bolometer angles. These atoms have been evaporated by the lower energy rotons so there are two obvious explanations: either the assumed energy distribution of incident rotons is incorrect, or the evaporation probability density  $p(q, \theta_h)$  increases with  $q$ .

Although the spectrum of high-energy phonons generated by thin-film heaters has been characterised<sup>10</sup> there have been no successful attempts to measure it independently for rotons. The simulation assumes that the number density  $n(q)$  of positive group-velocity rotons generated with wave vector  $q$  is

$$n(q) dq \propto \frac{q^\lambda dq}{\exp(E(q)/T_{\text{eff}}) - 1} \quad \text{where } \lambda = 2 \quad (5)$$

and that the evaporation probability  $p(q, \theta_h)$  is constant. The shape of  $n(q)$  is dominated by the value of the parameter  $T_{\text{eff}}$  and is insensitive to the density-of-states parameter for values  $1 < \lambda < 3$ . The value of  $T_{\text{eff}}$  is selected to fit the time-of-flight measurements; it increases with heater power and lies within the range 1.0K

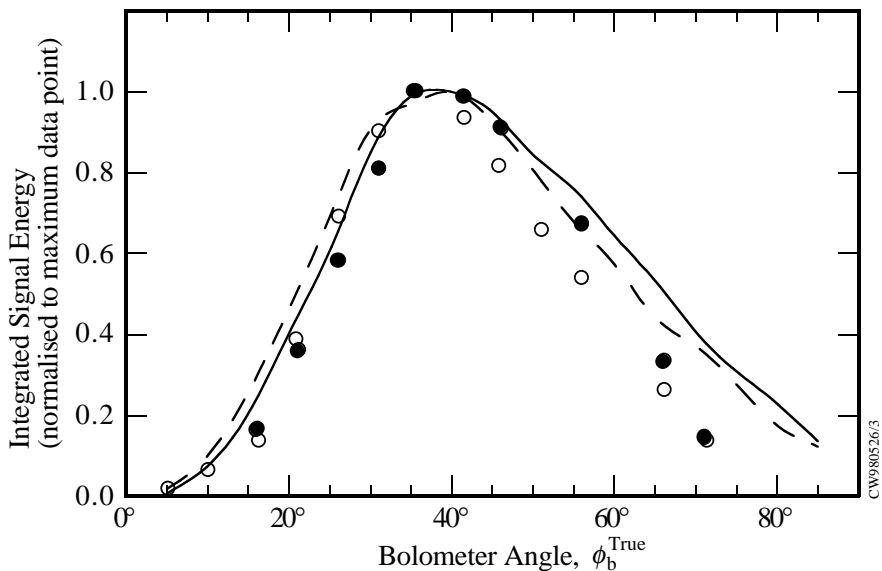


Fig. 5. The angular dependence of the integrated  $R^+ \rightarrow$  atom signal energy when  $\theta_h = 14^\circ$ . The signals are integrated up to  $160 \mu\text{s}$  after the start of the heater input pulse. The points are experiments using two different heater powers,  $-24 \text{ dB}$  (open circles) and  $-27 \text{ dB}$  (full circles). The curves are simulations using injected-roton spectra at two characteristic temperatures,  $T_{\text{eff}} = 1.0 \text{ K}$  (unbroken) and  $T_{\text{eff}} = 1.5 \text{ K}$  (dashes).

to 1.5 K. Simulations show that no reasonable combination of values of  $T_{\text{eff}}$  and  $\lambda$  fits the data so, either something is *dramatically* wrong with the form of equation 5 or, more likely, the probability of roton-atom evaporation is wave-vector dependent.

A BW-type of experiment is unable to determine absolute roton-atom quantum evaporation probabilities because the magnitude of  $n(q)$  is unknown. However, the angle of refraction  $\phi_b$  decreases quite markedly with increasing roton wave-vector and therefore figure 5 seems to suggest that the roton-atom evaporation probability increases with increasing wave-vector. The possibility of extracting some information about the wave-vector and angle dependence of quantum evaporation will be discussed in more detail elsewhere<sup>16</sup>.

## 5. RIPPLON PRODUCTION

If ripples are created as part of the quantum evaporation process then equations 1 and 2 will not be exact (they make no provision for the energy and momentum required to create the surface excitations) and the angular distribution and time-of-flight of the out-going atoms will be affected. The limits calculated by BW for the most likely processes can be reduced in the light of the improved simulations. If ripples were to be created singly then the angular distribution of atoms would be broadened and/or offset from the simulation. For phonons at near-normal incidence any such effect is no more than  $\sim 2^\circ$  (figure 3) so the BW limit on the ripple wave vectors can be reduced to  $q < 0.01 \pm 0.01 \text{ \AA}^{-1}$ . If ripples were created in pairs, with zero total momentum, there would be less broadening and it would be largest for phonons incident nearly parallel to the surface. With  $\theta_h = 75^\circ$  the peak in the phonon-atom signal is within  $\sim 2^\circ$  of the simulation, so ripples created by pair-production are limited to wave vectors of  $q < 0.07 \text{ \AA}^{-1}$  each.

The mysterious early first-arrival times of phonon-evaporated atoms described by BW are now understood; high-energy phonons are created some distance in front of the heater by an up-scattering process<sup>10</sup>. In practice this means that it is not prudent to rely on time-of-flight methods to reduce the limits further. The roton-atom arrival times are not affected in the same way and the BW conclusion that there is no evidence that ripples are involved in the evaporation process remains valid.

## 6. SUMMARY AND CONCLUSIONS

This paper confirms the original work of BW and brings many of their measurements into quantitative agreement with the description quantum evaporation presented in section 1. A pulse-heated thin film is now known to produce a narrow angular distribution of phonons and this brings the simulation into agreement with experiments for phonons at nearly normal incidence. Correcting the liquid level for

capillary effects brings the glancing angle phonon-evaporation signals into agreement. For phonons, where the energy range that causes evaporation is very narrow, there is no remaining discrepancy between simulation and experiment and no evidence for angular broadening due to ripplon production.

The roton-atom evaporation measurements have a feature that allows the angular error in the apparatus to be almost entirely attributed to the bolometer position, thereby removing an important previous source of uncertainty in interpretation. Even when all these corrections are included, the roton-evaporation measurements differ significantly from the simulation. The most likely reason is that the positive group-velocity roton-atom evaporation probability increases with wave-vector whereas the simulations treat it as a constant.

## ACKNOWLEDGMENTS

I am grateful to R.M. Bowley, M.A.H. Tucker and A.F.G. Wyatt for stimulating comments and discussions, and to EPSRC for support.

## REFERENCES

1. P.W. Anderson, *Phys. Lett.* **29A**, 563 (1969).
2. M.G. Brown and A.F.G. Wyatt, *J. Phys. Condens. Matter* **2**, 5025 (1990).
3. C. Enss, S.R. Bandler, R.E. Lanou, H.J. Maris, T. More, F.S. Porter and G.M. Seidel, *Physica B* **194**, 515 (1994).
4. A.C. Forbes and A.F.G. Wyatt *J. Low Temp. Physics* **101**, 537 (1995).
5. M.A.H. Tucker and A.F.G. Wyatt, *Czech. J. Physics* **46**, 263 (1996).
6. F. Dalfovo, A. Fracchetti, A. Lasteri, L. Pitaevskii and S. Stringari,, *J. Low Temp. Physics* **104**, 367 (1996) and references therein.
7. M.B. Sobnack, J.C. Inkson and F.C.H. Fung, *Czech. J. Physics* **46**, 393 (1996).
8. C.E. Campbell, E. Krotscheck and M. Saarela, *Phys. Rev. Lett.* **80**, 2169 (1998).
9. M. Brown, *Ph.D. Thesis*, University of Exeter (1990).
10. M.A.H. Tucker and A.F.G. Wyatt, *J. Phys. Condens. Matter* **6**, 2813 & 2825 (1994).
11. M. Guilleumas, F. Dalfovo, I. Oberosler, L. Pitaevskii and S. Stringari, *J. Low Temp. Physics* **110**, 449 (1998).
12. M.B. Sobnack and J.C. Inkson, *submitted to Phys. Rev. B.* (1998).
13. L.D. Landau and E.M. Lifshitz, *Fluid Mechanics, 2nd edn* chapter 7 (1987).
14. M. Iino, M. Suzuki and A.J. Ikushima, *J. Low Temp. Phys.* **61**, 155 (1985), K. Nakanishi and M. Suzuki, *J. Low Temp. Physics* (to be published) (1998).
15. H.M. Princen, *J. Colloid Interf. Sci.* **30**, 69 (1969).
16. C.D.H. Williams, *J. Low Temp. Physics* (to be published) (1998).